Electronic Supplementary Information

Synthesis, photophysical and mechanochromic properties of novel 2,3,4,6-tetraaryl-4*H*-pyran derivatives

Yufeng Xie, Zhiqiang Wang, Xiaoqing Liu, Miaochang Liu, Yunxiang Lei,* Yunbing Zhou, Wenxia Gao, Xiaobo Huang* and Huayue Wu*

College of Chemistry and Materials Engineering, Wenzhou University, Wenzhou 325035, P. R. China

E-mail: 173612907@qq.com (Y. Lei), xiaobhuang@wzu.edu.cn (X. Huang), huayuewu@wzu.edu.cn (H. Wu)

Contents:

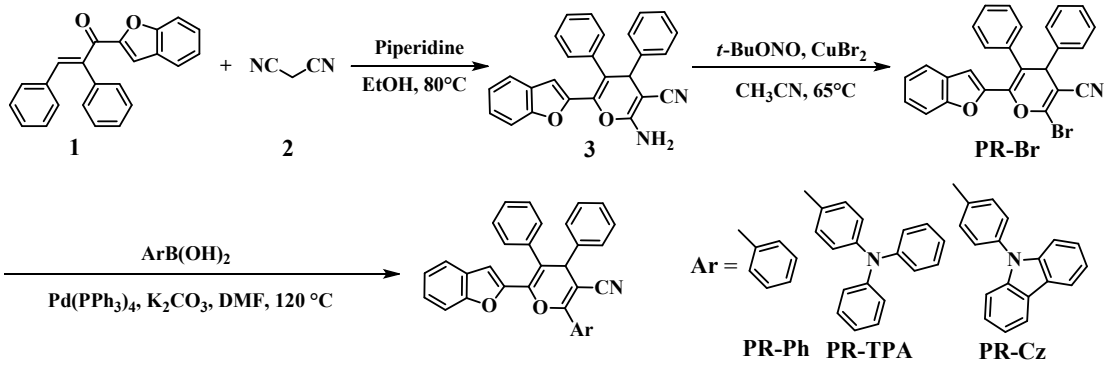

Scheme S1 Synthetic routes of **PR-Ph**, **PR-TPA**, and **PR-Cz**.

1. Experimental

Measurements and materials

NMR spectra were determined using a Bruker DRX 500 NMR spectrometer using dimethyl sulfoxide (DMSO-d_6) or tetrahydrofuran (THF-d_8) as a solvent and trimethylsilane as a reference. Melting points were determined on a WRS-1B digital melting point meter and were uncorrected. HRMS-ESI mass spectra were conducted on a Hitachi Nano Frontier LD spectrometer. UV-vis absorption spectra were performed with a UV-3600 Shimadzu spectrophotometer. Fluorescence spectra were performed with a HITACHI F-7000 fluorometer. The absolute fluorescence quantum yields and fluorescence lifetime decays were performed using a Jobin Yvon Horiba FluoroMax-4 fluorometer. The X-ray powder diffraction (XRD) data were conducted on a Bruker X-ray diffractometer. The measurements of the average particle sizes of the aggregates in solution were determined using a Zetasizer Nano ZS Laser Particle Size Analyzer. Differential scanning calorimetry (DSC) experiments were obtained using a TA-DSC Q2000 at a heating rate of 10 °C/min. The X-ray crystallographic analyses were conducted on a Bruker SMART II CCD area detector. (*E*)-1-(Benzofuran-2-yl)-2,3-diphenylprop-2-en-1-one (**1**) was synthesized according to the previous report.[1] Malononitrile (**2**), piperidine, *tert*-butyl nitrite, and various aromatic boric acids were purchased from commercial suppliers.

Synthesis of 2-amino-6-(benzofuran-2-yl)-4,5-diphenyl-4*H*-pyran-3-carbonitrile (3)

A mixture of compound **1** (0.81 g, 2.5 mmol), compound **2** (0.33 g, 5.0 mmol), piperidine (0.21 g, 2.5 mmol), and ethyl alcohol (10 mL) was heated at 80°C for 1.5 h. After cooling to the room temperature, a large amount of solids separated out. After vacuum filtration, the crude product was washed with ethyl alcohol three times and then afforded compound **3**. White solid (0.63 g), 64.6% yield, m. p. 238.8-229.6°C. ^{1}H NMR (DMSO-d_6, 500 MHz): δ 7.55 (d, J = 8.0 Hz, 1H), 7.31-7.26 (m, 4H), 7.21-7.16 (m, 7H), 7.02-7.00 (m, 4H), 6.61 (s, 1H), 4.41 (s, 1H) ppm. ^{13}C NMR (DMSO-

d_6, 125 MHz): δ 159.6, 153.6, 148.1, 143.2, 136.5, 135.6, 128.8, 128.5, 128.0, 127.7, 127.6, 127.03, 126.98, 125.3, 123.2, 121.4, 119.9, 110.9, 107.4, 57.1, 45.0 ppm. HRMS (ESI) m/z: $[M+H]^+$ calculated for $C_{26}H_{19}N_2O_2$, 391.1441; found, 391.1442.

Synthesis of 6-(benzofuran-2-yl)-2-bromo-4,5-diphenyl-4*H*-pyran-3-carbonitrile (PR-Br)

A mixture of compound **3** (0.98 g, 2.5 mmol), *tert*-butyl nitrite (0.52 g, 5.0 mmol), copper (II) bromide (0.72 g, 5.0 mmol), and acetonitrile (10 mL) was heated at 65°C for 30 min. After cooling to the room temperature, a large amount of solids separated out. The crude product was obtained by vacuum filtration and then purified by a silica gel column chromatography using petroleum ether/ethyl acetate (v:v = 20:1) as the eluent to give pure **PR-Br**. Yellow solid (0.30 g), 26.4% yield, m. p. 175.5-176.2°C. ^{1}H NMR (DMSO-d_6, 500 MHz): δ 7.55 (d, J = 8.0 Hz, 1H), 7.38-7.35 (m, 3H), 7.32-7.28 (m, 4H), 7.26-7.20 (m, 4H), 7.04 (d, J = 7.5 Hz, 2H), 6.55 (s, 1H), 4.84 (s, 1H) ppm. ^{13}C NMR (DMSO-d_6, 125 MHz): δ 153.7, 146.4, 139.99, 139.96, 137.4, 135.0, 129.0, 128.7, 128.4, 128.3, 128.2, 128.1, 127.0, 126.9, 125.8, 123.4, 121.7, 118.7, 116.7, 111.1, 108.3, 95.1, 46.3 ppm. HRMS (ESI) m/z: $[M+H]^+$ calculated for $C_{26}H_{17}BrNO_2$, 454.0437; found, 454.0467.

General procedure for PR-Ph, PR-TPA and PR-Cz.

A mixture of **PR-Br** (2.5 mmol), phenylboronic acid/(4-(diphenylamino)phenyl)boronic acid/ (4-(9*H*-carbazol-9-yl)phenyl)boronic acid (5.0 mmol), K_2CO_3 (5.0 mmol), $Pd(PPh_3)_4$ (1 mol %), and DMF (10 mL) was stirred at 120°C under nitrogen for 12 h. The reaction mixture was extracted with CH_2Cl_2 (50 mL×3). The organic layer was washed with water and then brine, dried over anhydrous Na_2SO_4, and then evaporated in vacuumto dryness. The residue was purified by a silica gel column chromatography using petroleum ether/ethyl acetate (v:v = 80:1) as the eluent to afford pure target compound.

6-(Benzofuran-2-yl)-2,4,5-triphenyl-4*H*-pyran-3-carbonitrile (PR-Ph). Pale yellow solid (0.80 g), 72.5% yield, m. p. 127.4-128.1 °C. ^{1}H NMR (DMSO-d_6, 500 MHz): δ 7.91 (d, J = 6.5 Hz, 2H), 7.63-7.57 (m, 4H), 7.40-7.35 (m, 4H), 7.31-7.20 (m, 7H), 7.08 (d, J = 6.5 Hz, 2H), 6.76 (s, 1H), 4.77 (s, 1H) ppm. ^{13}C NMR (DMSO-d_6, 125 MHz): δ 158.9, 153.7, 147.8, 141.4, 136.8, 135.9, 131.6,130.8, 129.0, 128.91, 128.85, 128.4, 128.2, 128.0, 127.9, 127.8, 127.2, 125.6, 123.4, 121.6, 118.1, 117.9, 111.1, 107.7, 88.7, 45.8 ppm. HRMS (EI) m/z: $[M]^+$ calculated for $C_{32}H_{21}NO_2$, 451.1572; found, 451.1567.

6-(Benzofuran-2-yl)-2-(4-(diphenylamino)phenyl)-4,5-diphenyl-4*H*-pyran-3-carbonitrile (PR-TPA). Pale yellow solid (1.28 g), 83.0% yield, m. p. 176.2-176.5 °C. ^{1}H NMR (THF-d_8, 500 MHz): δ 7.92 (d, J = 8.5 Hz, 2H), 7.46 (d, J = 7.5 Hz, 1H), 7.36-7.05 (m, 25H), 6.68 (s, 1H), 4.47 (s, 1H) ppm. ^{13}C NMR (THF-d_8, 125 MHz): δ 159.2, 155.5, 151.6, 149.8, 147.9, 143.1, 138.8, 138.0, 130.4, 130.0, 129.8, 129.7, 129.2, 129.0, 128.7, 128.6, 128.5, 126.6, 126.0, 125.1, 124.4, 123.9, 122.1, 121.4, 119.2, 119.0, 111.9, 108.1, 88.0, 48.5 ppm. HRMS (ESI) m/z: $[M+Na]^+$

calculated for $C_{44}H_{30}N_2O_2Na$, 641.2205; found, 641.2209.

2-(4-(9*H*-Carbazol-9-yl)phenyl)-6-(benzofuran-2-yl)-4,5-diphenyl-4*H*-pyran-3-carbonitrile (PR-Cz). Pale yellow solid (1.25 g), 81.2% yield, m. p. 119.2-122.5 °C. ^{1}H NMR (DMSO-d_6, 500 MHz): δ 8.28 (d, J = 7.5 Hz, 2H), 8.23 (d, J = 8.5 Hz, 2H), 7.90 (d, J = 8.0 Hz, 2H), 7.60 (d, J = 7.5 Hz, 1H), 7.53-7.46 (m, 4H), 7.41-7.40 (m, 4H), 7.35-7.31 (m, 4H), 7.28-7.21 (m, 5H), 7.13-7.11 (m, 2H), 6.85 (s, 1H), 4.84 (s, 1H) ppm. ^{13}C NMR (DMSO-d_6, 125 MHz): δ 157.8, 153.7, 147.8, 141.3, 139.6, 136.8, 135.8, 129.6, 129.2, 129.0, 128.8, 128.4, 128.2, 128.0, 127.9, 127.1, 126.6, 126.4, 125.5, 123.3, 123.1, 121.6, 120.5, 118.0, 117.9, 111.0, 109.7, 107.7, 88.8, 45.7 ppm. HRMS (ESI) m/z: $[M+Na]^+$ calculated for $C_{44}H_{28}N_2O_2Na$, 639.2049; found, 639.2043.

Lippert-Mataga plots of PR-TPA and PR-Cz in organic solvents

The effect of solvent polarity on the optical properties of **PR-TPA** and **PR-Cz** are investigated by Lippert-Mataga equation listed as follows: $\Delta\nu = 2(\mu_e-\mu_g)^2\Delta f/hca^3+C$, which describes the interactions between the solvent and the dipole moment of a fluorescent molecule.[2] Herein, $\Delta\nu$ is Stokes shifts of the fluorescent molecule based on the equation: $\Delta\nu = \nu_{abs}-\nu_{em}$. μ_g and μ_e are the dipole moments in the ground state and the excited state, respectively. h and c are the Planck constant and the speed of light, respectively, and a is the radius of the fluorescent molecule. Δf is the solvent polarity parameter of solvent, which is obtained from the following equation: $(\varepsilon-1)/(2\varepsilon+1)-(n^2-1)/(2n^2+1)$, herein, ε and n are the dielectric constant and refractive index of the solvent, respectively. Δf values for the various solvents are calculated from known values of ε and n. The dependence of the $\Delta\nu$ values of **PR-TPA** and **PR-Cz**, which are obtained from on the emission and absorption spectra in different solvents, on the solvent polarity parameter Δf are fitted to linear function, providing the Lippert-Mataga plots of **PR-TPA** and **PR-Cz**.

References

1. L. Shan, G. Wu, M. Liu, W. Gao, J. Ding, X. Huang, H. Wu, *Org. Chem. Front.*, 2018, **5**, 1651–1654.
2. (a) J. R. Lakowicz, Principles of fluorescence spectroscopy. New York: Plenum Press; 1983. p. 190; (b) H. Li, Y. Guo, Y. Lei, W. Gao, M. Liu, J. Chen, Y. Hu, X. Huang and H. Wu, *Dyes Pigm.*, 2015, **112**, 105–115.

2. Figures and tables

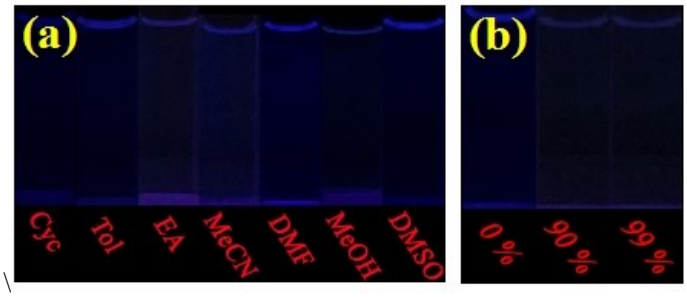

Fig. S1 (a) Fluorescence photos of **PR-Ph** in different solvents at a concentration of 1×10^{-5} mol/L under UV irradiation (365 nm). (b) Fluorescence photos of **PR-Ph** in the THF-water mixtures (1×10^{-5} mol/L) at f_w = 0, 90%, and 99% under UV irradiation (365 nm).

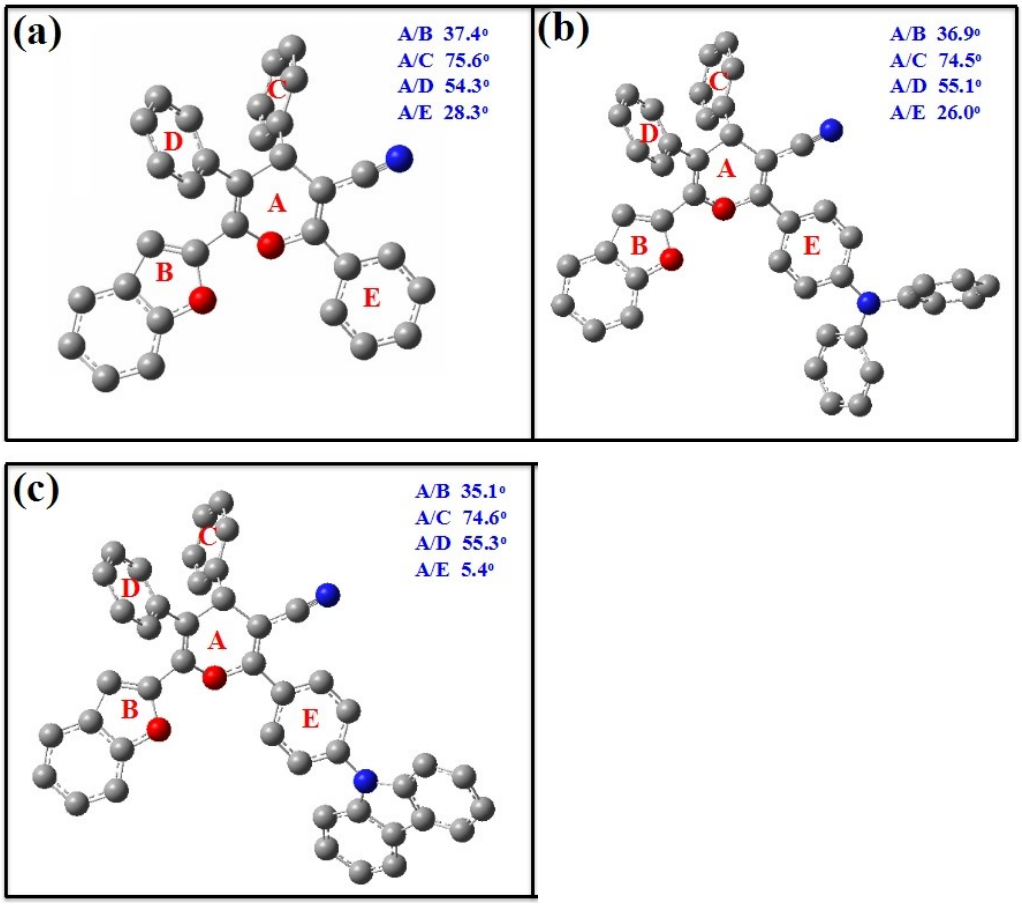

Fig. S2 The optimized molecular conformations and the dihedral angles of **PR-Ph** (a), **PR-TPA** (b), and **PR-Cz** (c) between the central 4*H*-pyran ring and the surrounding aromatic rings by the calculation using the B3LYP/6-311+G** basis set.

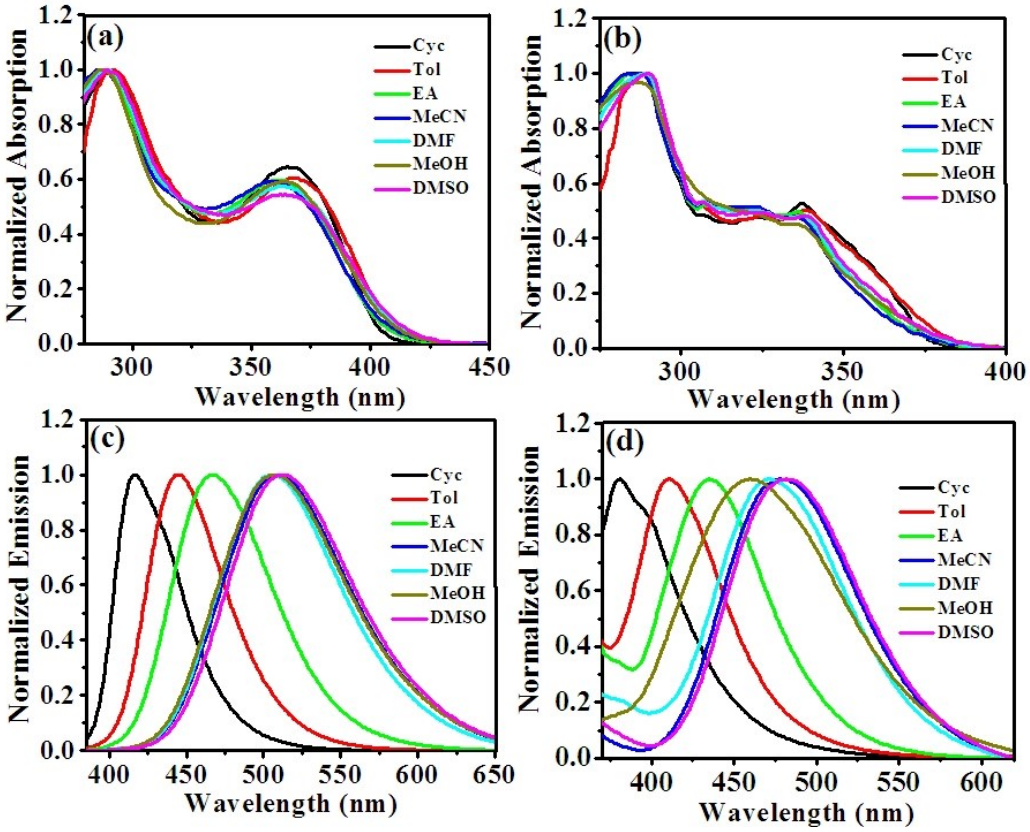

Fig. S3 Normalized absorption and fluorescence spectra of **PR-TPA** (a, c) and **PR-Cz** (b, d) in different solvents at a concentration of 1×10^{-5} mol/L.

Table S1 UV-vis absorption maxima and fluorescence emission maxima of **PR-TPA** and solvent polarity parameter in different solvents

	Cyc	Tol	EA	DMSO	DMF	MeCN	MeOH
λ_{abs}/nm	366	368	362	364	363	359	364
ν_{abs}/cm^{-1}	27322	27174	27624	27473	27548	27855	27473
λ_{ex}/nm	368	370	366	365	367	366	367
λ_{em}/nm	416	445	457	513	506	509	507
ν_{em}/cm^{-1}	24038	22472	21413	19493	19763	19646	19724
$\Delta\nu$/cm^{-1}	3284	4702	6211	7979	7785	8209	7749
Δf	-0.151	0.0135	0.2	0.263	0.276	0.305	0.308

Table S2 UV-vis absorption maxima and fluorescence emission maxima of **PR-Cz** and solvent polarity parameter in different solvents

	Cyc	Tol	EA	DMSO	DMF	MeCN	MeOH
λ_{abs}/nm	337	338	336	338	337	335	336
ν_{abs}/cm^{-1}	29674	29586	29762	29586	29674	29851	29762
λ_{ex}/nm	338	339	335	334	336	335	337
λ_{em}/nm	380	410	435	482	471	477	460
ν_{em}/cm^{-1}	26316	24390	22989	20747	21231	20921	21739
$\Delta\nu$/cm^{-1}	3358	5196	6773	8839	8443	8930	8023
Δf	-0.151	0.0135	0.2	0.263	0.276	0.305	0.308

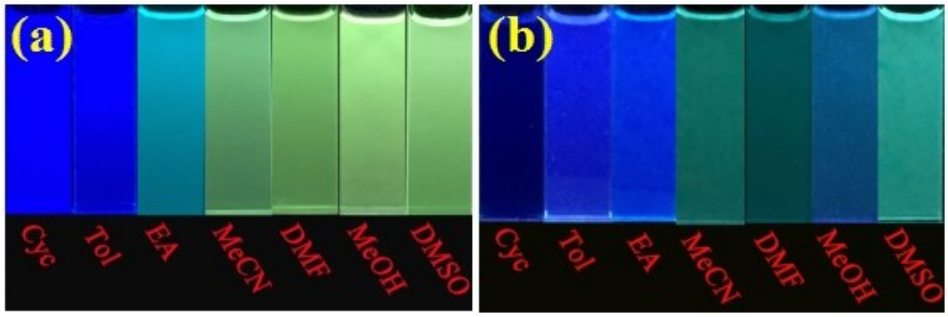

Fig. S4 Fluorescence photos of **PR-TPA** (a) and **PR-Cz** (b) in different solvents at a concentration of 1 × 10^{-5} mol/L) under UV irradiation (365 nm).

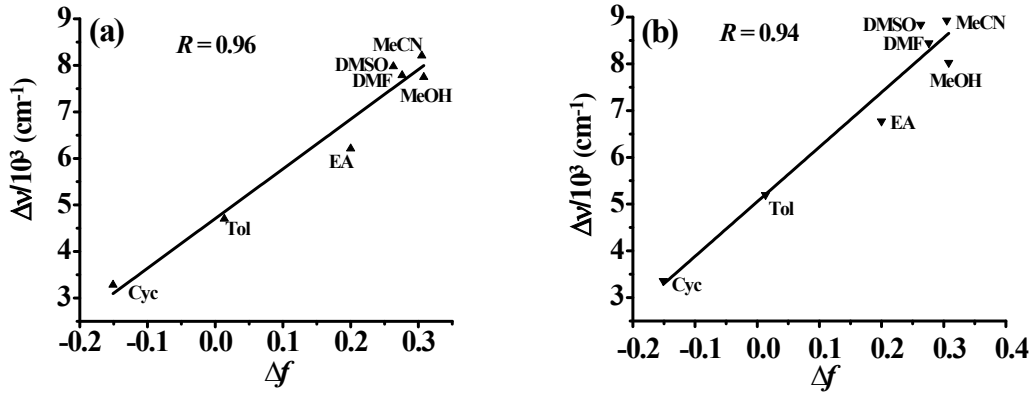

Fig. S5 Lippert-Mataga plots of Stokes shifts ($\Delta\nu$) of **PR-TPA** (a) and **PR-Cz** (b) *vs* solvent polarity parameter (Δf) in various solvents.

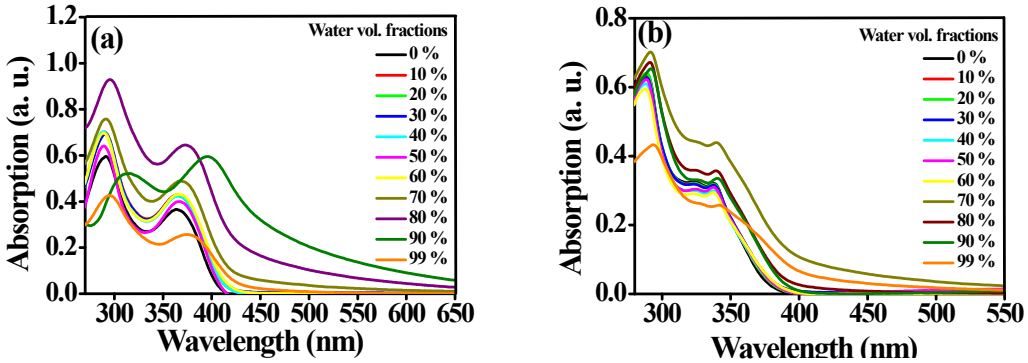

Fig. S6 UV-vis absorption of **PR-TPA** (a) and **PR-Cz** (b) in THF-water mixtures (1×10^{-5} mol/L) with different f_w values.

Table S3 Average particle size and polydispersity index (PDI) of **PR-TPA** and **PR-Cz** in THF-water mixtures with different f_w.

Compound	f_w	Average particle size (nm)	PDI
PR-TPA	70%	349	0.120
	80%	304	0.197
	90%	171	0.195
	99%	293	0.250
PR-Cz	80%	338	0.114
	90%	149	0.246
	99%	181	0.191

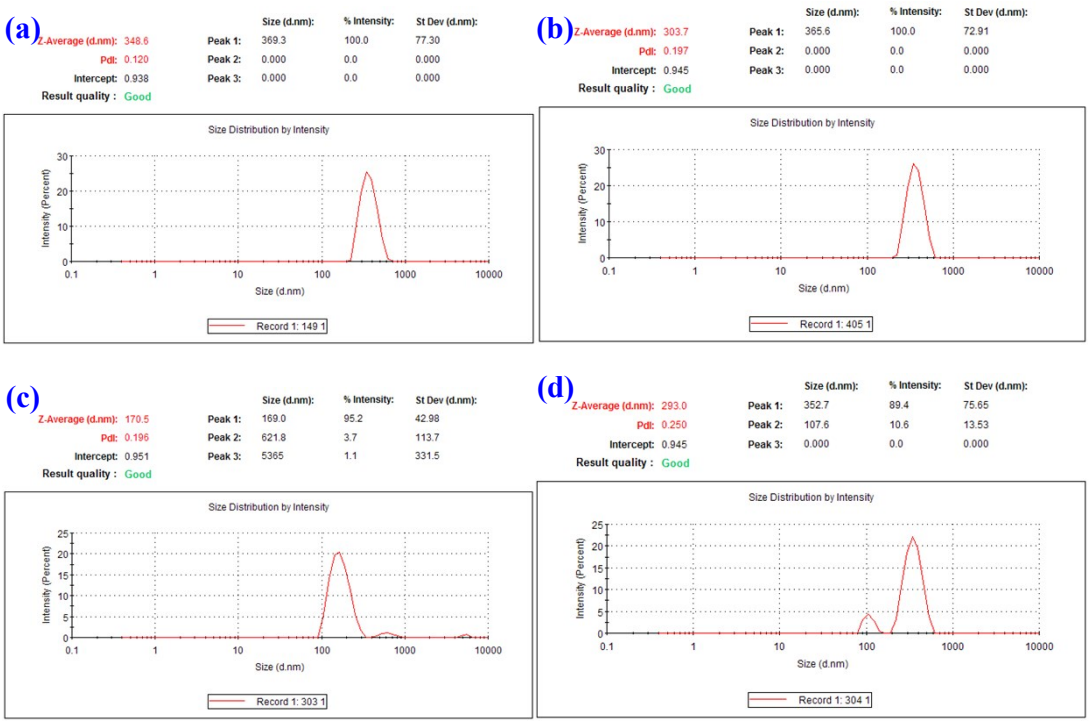

Fig. S7 The average particle size and PDI of **PR-TPA** in THF-water mixture with f_w = 70% (a),

80% (b), 90% (c), and 99% (d), respectively.

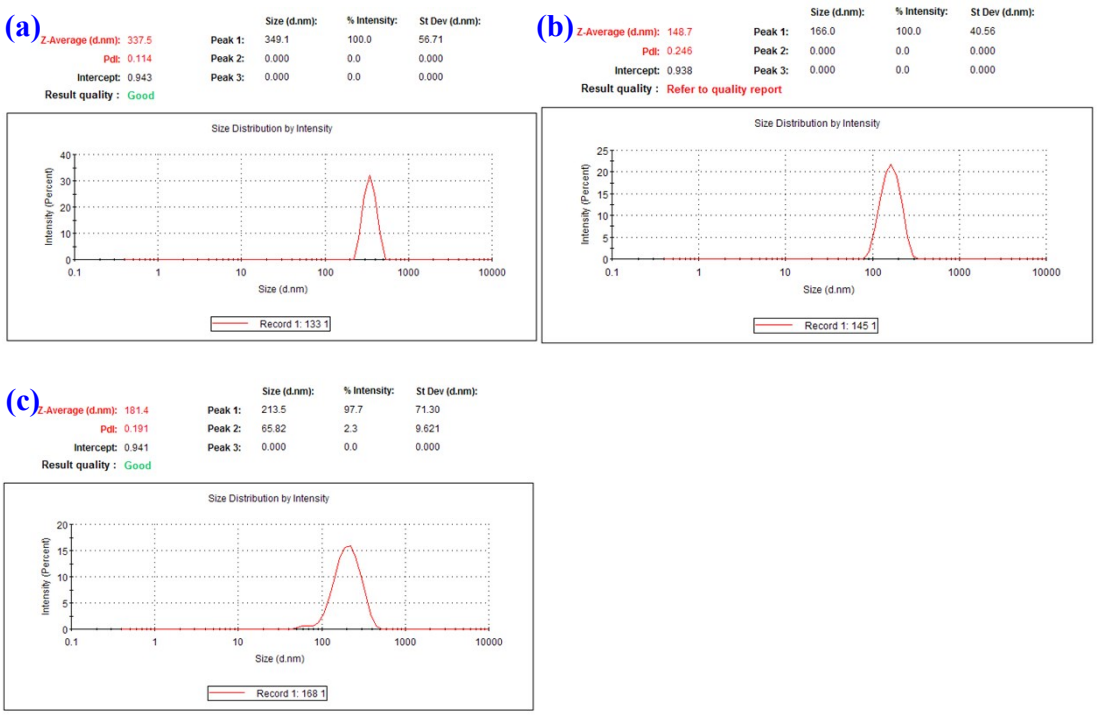

Fig. S8 The average particle size and PDI of **PR-Cz** in THF-water mixture with f_w = 80% (a), 90% (b), and 99% (c), respectively.

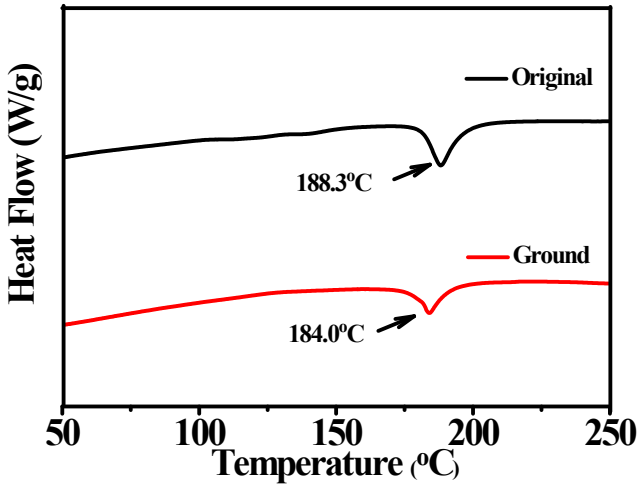

Fig. S9 DSC curves of the original sample of **PR-TPA** before and after grinding.

Table S4 Crystallographic data of the single crystals of **PR-Br** and **PR-TPA**

	PR-Br	**PR-TPA**
CCDC (No.)	2016180	2016181
Empirical formula	$C_{26}H_{16}BrNO_2$	$C_{44}H_{30}N_2O_2$
Formula weight	454.31	618.70
Temperature (K)	293(2)	216.58
Crystal system	Monoclinic	Monoclinic
Space group	*P* 2(1)/*c*	*P*$\bar{1}$ 2(1)/*c* 1
Z	4	4
D_{calcd} [Mg/m^3]	1.435	1.063
F (000)	920	1296
θ range [°]	2.734-25.998	2.421-24.999
R_1 [I>2σ(I)]	0.0346	0.0676
wR_2 [I>2σ(I)]	0.0818	0.1593
a [Å]	9.6941(3)	21.061(2)
b [Å]	18.5267(5)	10.0830(12)
c [Å]	11.8970(3)	19.630(2)
α [deg]	90	90
β [deg]	100.2540(10)	111.986(4)
γ [deg]	90	90
V [Å^3]	2102.57(10)	3865.4(7)
GOF	1.034	0.990
R (int)	0.0346	0.0956
No. of reflcns collected	22758	34215
No. of unique reflcns	4116	6778
R_1 (all data)	0.0525	0.1270
wR_2 (all data)	0.0907	0.2003

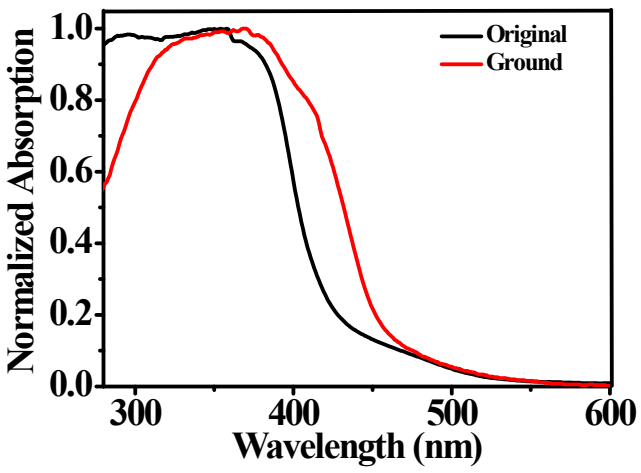

Fig. S10 Absorption spectra of the orginal and ground samples of **PR-TPA**.

3. Spectra of NMR

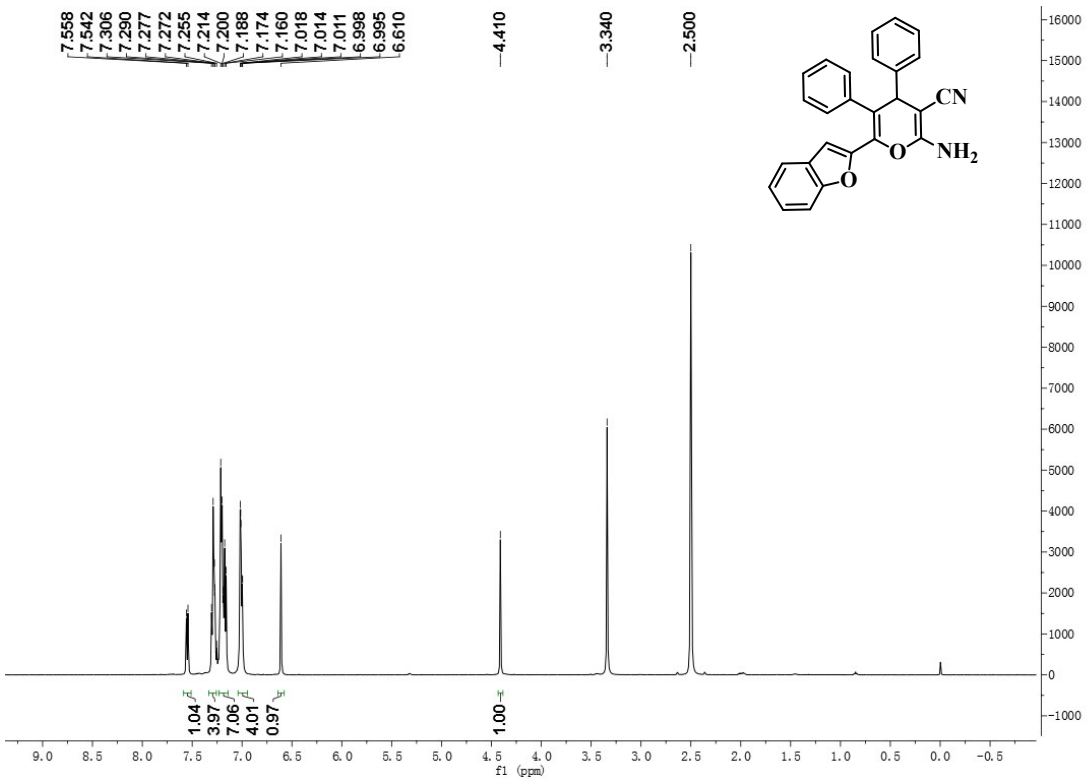

Fig. S11 ^{1}H NMR of compound **3** (DMSO-d_6, 500 MHz).

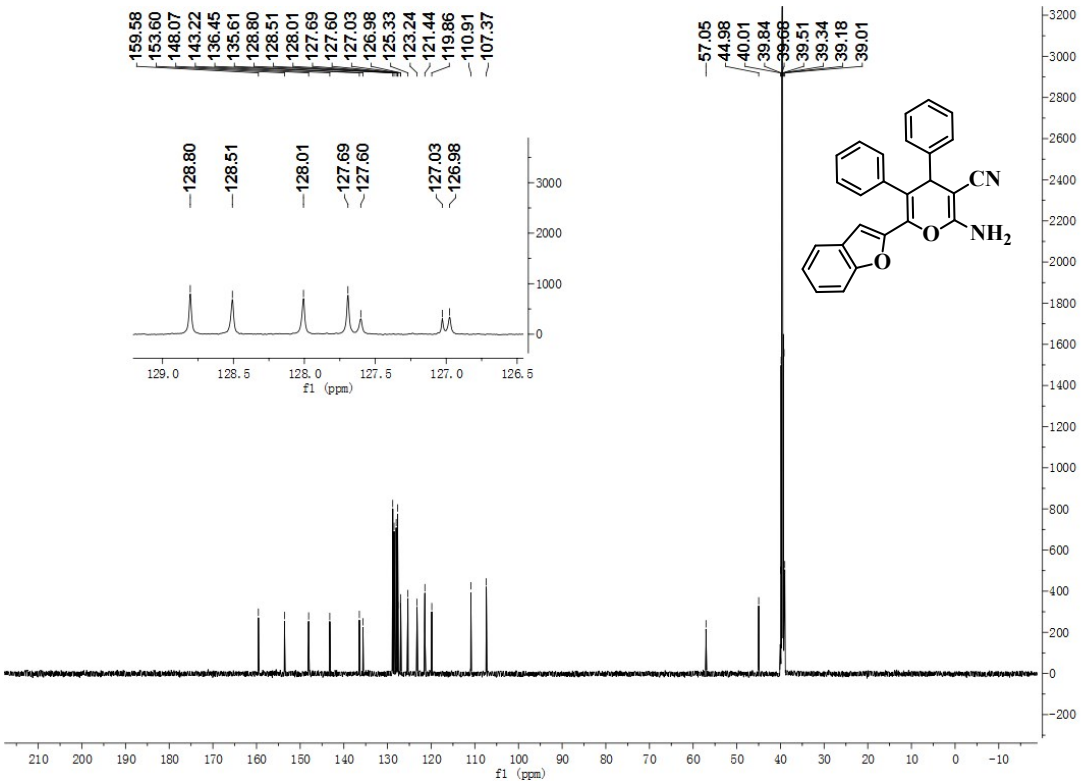

Fig. S12 ^{13}C NMR of compound **3** (DMSO-d_6, 125 MHz).

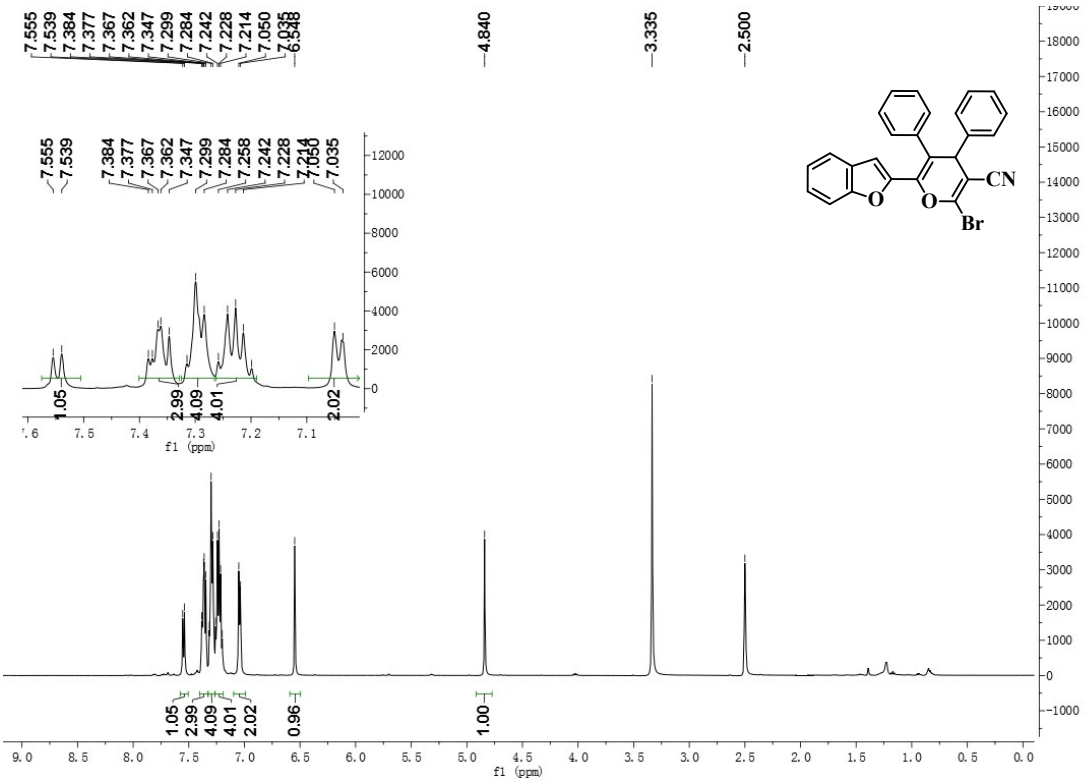

Fig. S13 ^{1}H NMR of **PR-Br** (DMSO-d_6, 500 MHz).

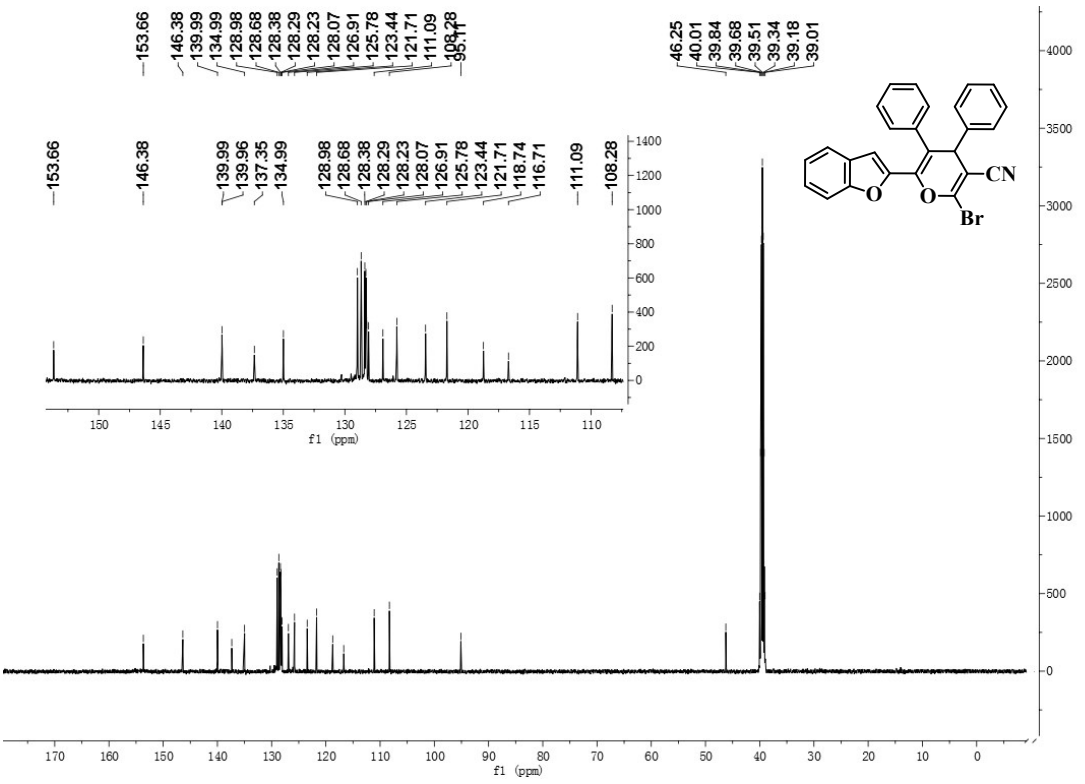

Fig. S14 ^{13}C NMR of **PR-Br** (DMSO-d_6, 125 MHz).

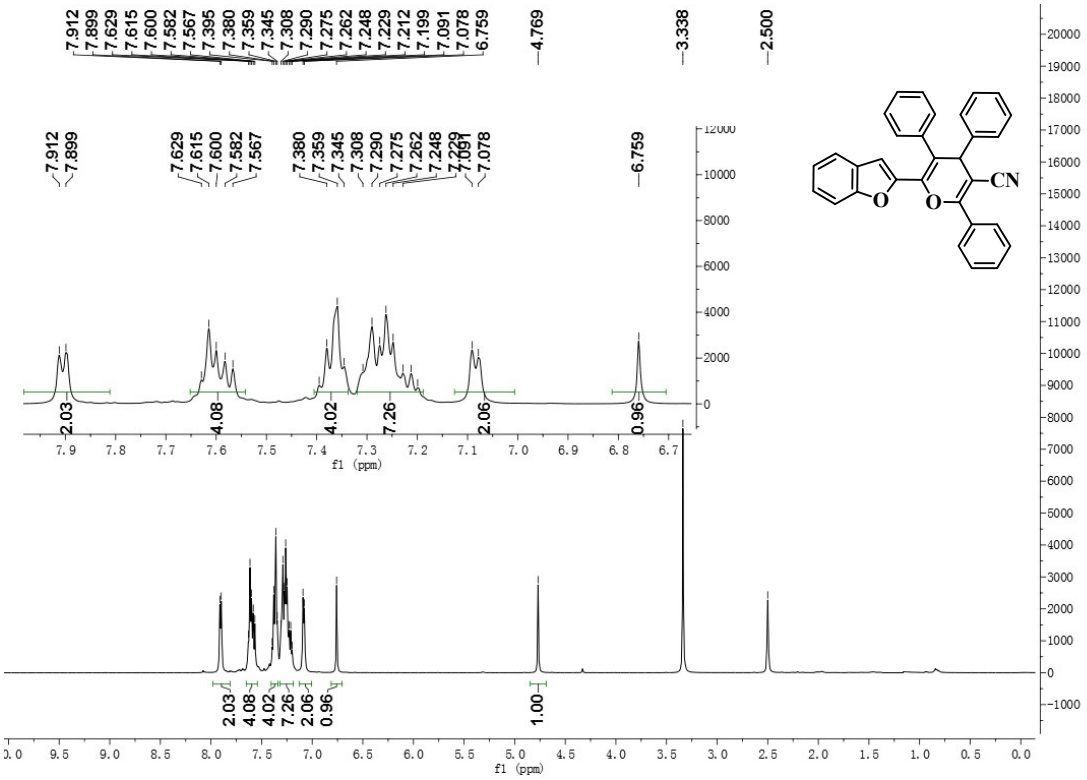

Fig. S15 ^{1}H NMR of **PR-Ph** (DMSO-d_6, 500 MHz).

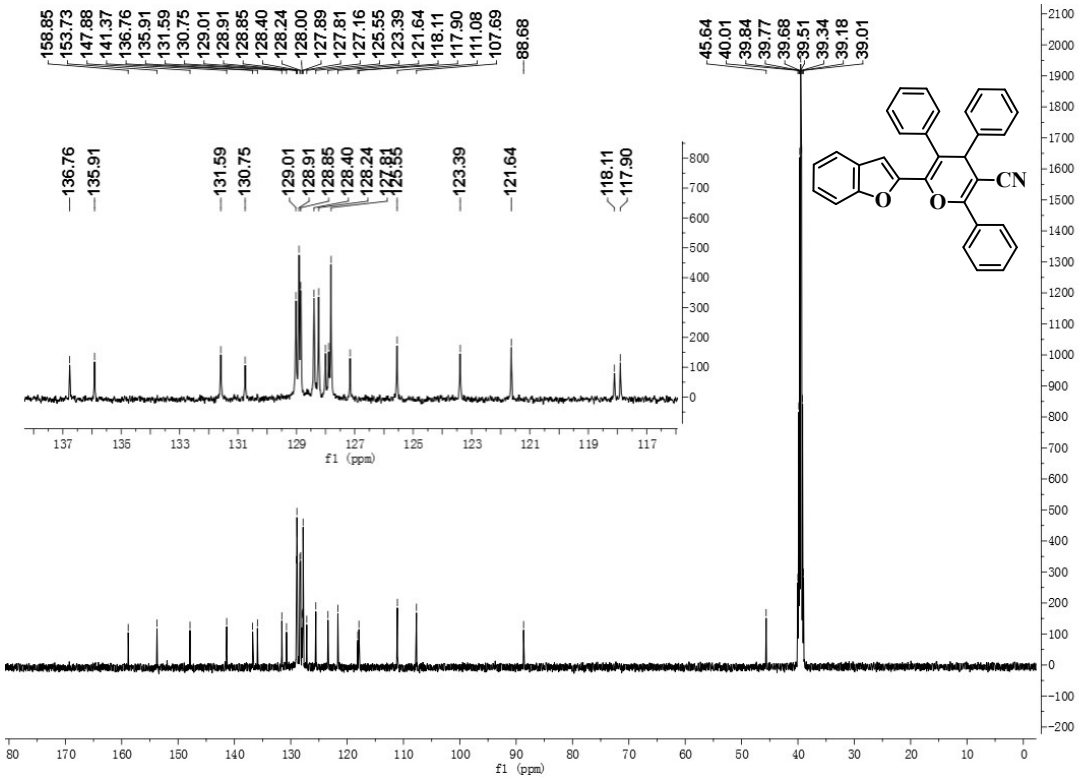

Fig. S16 ^{13}C NMR of **PR-Ph** (DMSO-d_6, 125 MHz).

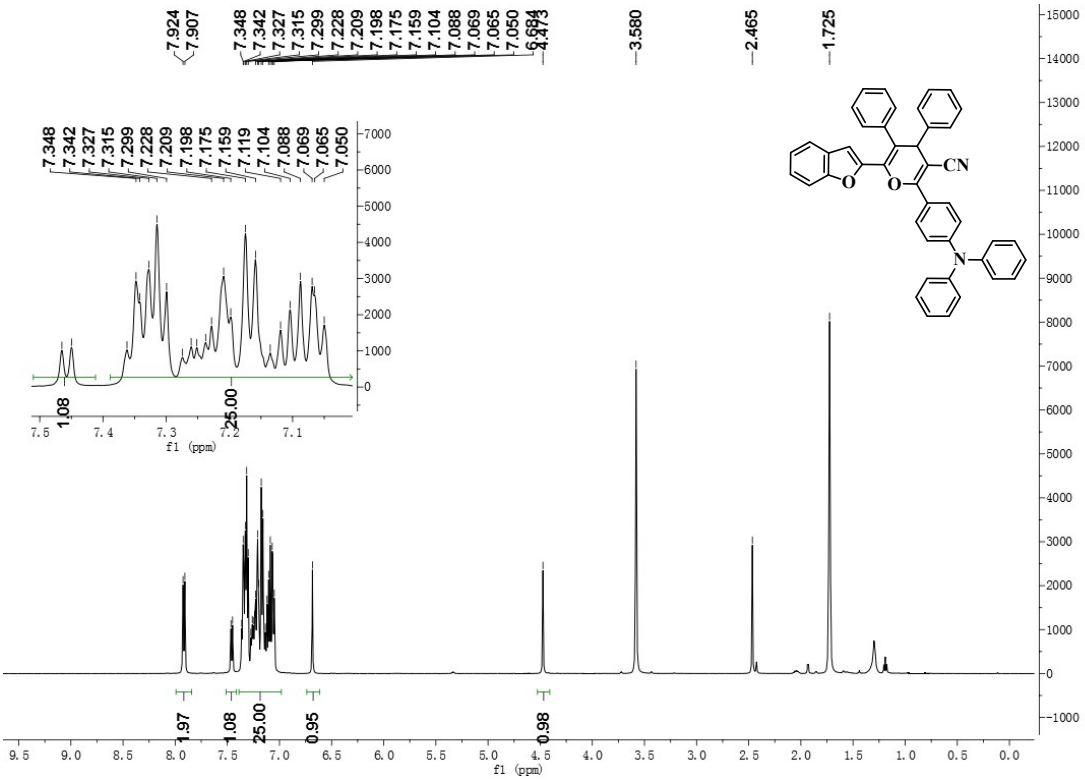

Fig. S17 ^{1}H NMR of **PR-TPA** (THF-d_8, 500 MHz).

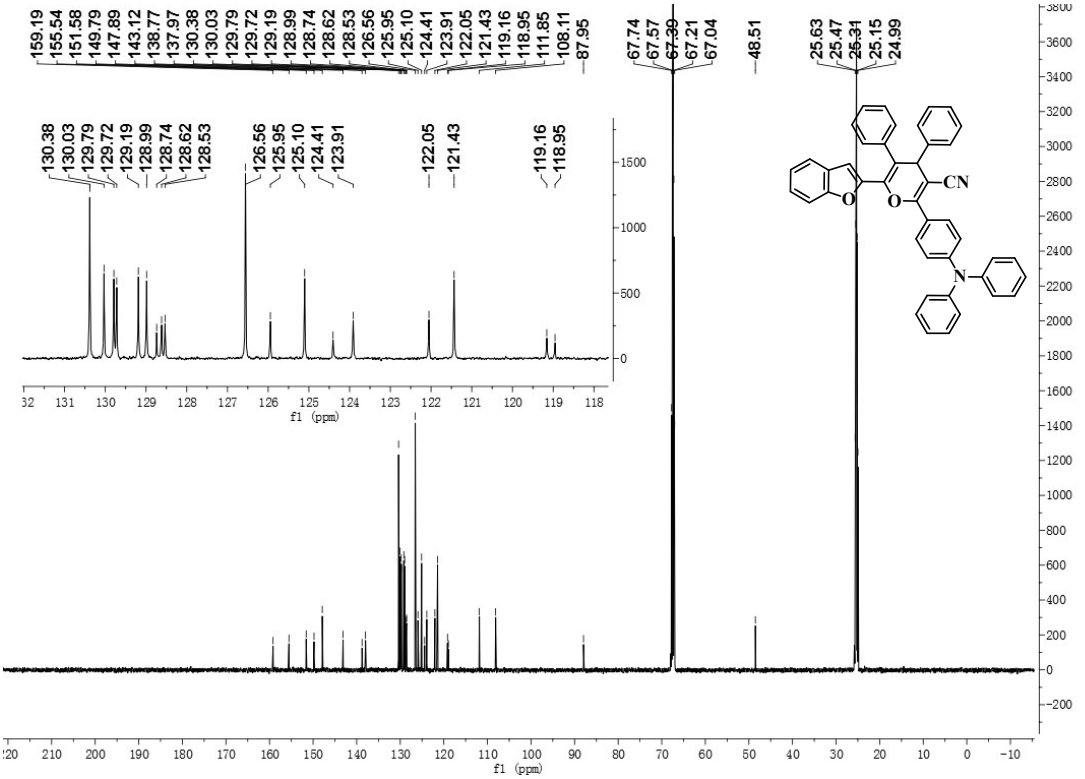

Fig. 18 ^{13}C NMR of **PR-TPA** (THF-d_8, 125 MHz).

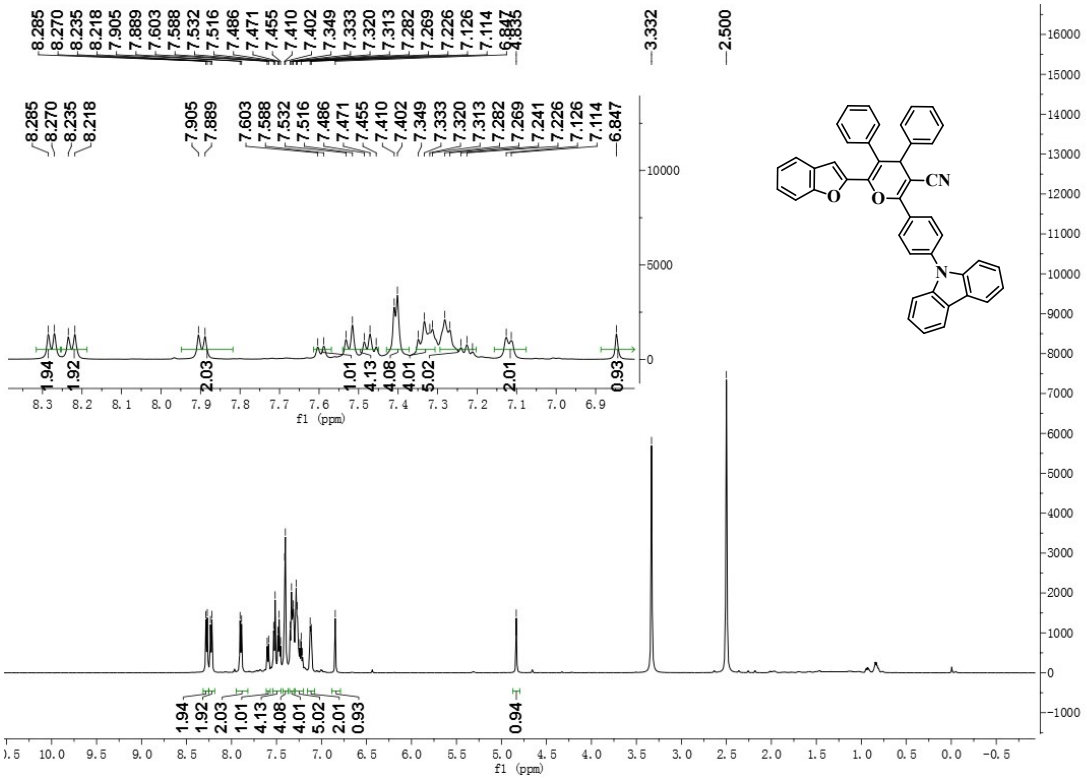

Fig. S19 ^{1}H NMR of **PR-Cz** (DMSO-d_6, 500 MHz).

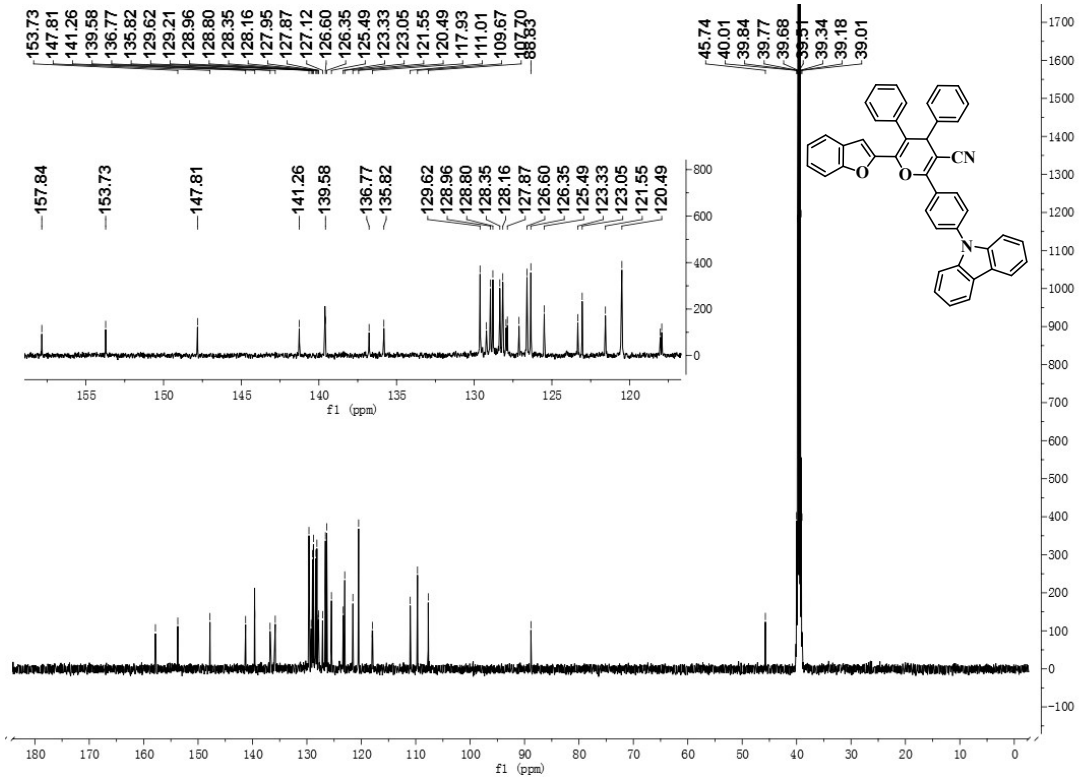

Fig. S20 ^{13}C NMR of **PR-Cz** (DMSO-d_6, 125 MHz).